9.1   ASYMMETRIC EYEWALL VERTICAL MOTION IN A HIGH-
            RESOLUTION SIMULATION OF HURRICANE BONNIE (1998)

Scott A. Braun, NASA/GSFC
Michael T. Montgomery, Colorado State University
Zhaoxia Pu, University of Maryland Baltimore County

1. Introduction

Heymsfield et al. (2001) described the structure of Hurricane Bonnie on August 23, 1998, using multiple observations from the NASA Convection And Moisture EXperiment (CAMEX-3). On that day, Bonnie's structure was highly asymmetric with strong low-level reflectivities on the eastern side of the storm and little precipitation on the western side. Observations from the NASA ER-2 Doppler radar indicated isolated deep convective towers on the eastern side of the storm with updrafts greater than 10 m s^{-1}. Heymsfield et al. (2001) developed a conceptual model for the evolution of the convective towers in which the updrafts formed near the top of the boundary layer on the southern side of the eyewall and grew progressively taller while moving around to the northern side. In other words, the convection was viewed in terms of rising plumes of air that were initiated to the south and reached the upper troposphere to the north of the eye.

This study examines a high-resolution simulation of Hurricane Bonnie. Results from the simulation will be compared to the conceptual model of Heymsfield et al. (2001) to determine the extent to which this conceptual model explains vertical motions and precipitation growth in the eyewall.

2. Methodology

The model used in this study is the PSU-NCAR non-hydrostatic fifth generation mesoscale model (MM5 V3.4). The simulation uses four levels of grid nesting starting at 36 km and then nesting to 12, 6, and 2 km. The simulation is started at 1200 UTC 22 August 1998 and run for 36 hours with only the 36- and 12-km grids active, with model output saved every hour. A one-way nest is used to conduct a higher resolution simulation on the 6- and 2-km grids starting at 6 h into the simulation. The higher resolution grids are run until 36 h with output every 15 min. A 6-h period from 24-30 h is run with output every 3 min. The 2 km grid was moved hourly to keep it centered on the storm. Physics options include a modified version of the Blackadar planetary boundary layer scheme in which parameterization of the surface roughness parameters follows Garratt (1998) and Pagowski and Moore (2001). Cloud processes are represented by the Grell cumulus parameterization scheme (on the 36- and 12-km grids only) and the Goddard cloud microphysics. Radiative processes are

Corresponding author: Dr. Scott Braun, NASA/GSFC, Code 912, Greenbelt, MD 20771, Scott.A.Braun@nasa.gov

calculated every five minutes.

Initial and boundary conditions were obtained from 12-hourly global ECMWF analyses archived at NCAR. Because the large-scale analysis does not contain an adequate representation of the initial hurricane vortex, a bogusing technique using four-dimensional variational data assimilation is used (Pu and Braun 2001). The assimilation was performed on the 36-km grid only.

3. Wavenumber 1 asymmetry in the eyewall

In this section, we investigate the time-averaged vertical motion and precipitation fields and the mechanisms that force the wavenumber 1 asymmetry. Figure 1 shows the 6-h averaged fields of vertical motion and total precipitation mixing ratio at four levels from the top of the boundary layer to the upper troposphere. The precipitation contours show that the maximum precipitation occurs on the northeastern side of the storm at all levels. In contrast, the vertical motions show some variation with height. At 1 km, the maximum upward motion is on the northeastern side of the storm just inside the region of maximum precipitation. At mid levels (5 and 8 km), the maximum upward motions occur on the southeastern side of the storm. At 12 km, the upward motions are much weaker with no clearly defined maximum. Downward motion is strongest at mid-to-upper levels and is concentrated in two areas: on the western side of the storm within or just outside the western portion of the eyewall and within the eye just inside the heavy precipitation associated with the eyewall.

Many studies have examined the impact of vertical wind shear on the development of wavenumber 1 asymmetries in the eyewall and have described several mechanisms by which this occurs. These include: (1) the tilting of adiabatic vortices by the shear and the subsequent development of upward motion in the downtilt direction as required for the flow to remain balanced (Jones 1995; Wang and Holland 1996); (2) the development of upward motion 90 degrees to the right of the tilt direction as a result of the interaction of the vortex flow with the temperature asymmetries generated by (1); and, (3) the effects of flow relative to the storm and an assumed balance between horizontal vorticity advection and vorticity stretching or compression that generally produces upward motion in the downshear direction (Bender 1997; Frank and Ritchie 2001). Expanding upon mechanism (1), Reasor et al. (2003) examined the tilting of a vortex by shear and found that a damping mechanism intrinsic to the dry adiabatic dynamics suppresses departures from an upright state. This realignment occurs through projection of the tilt
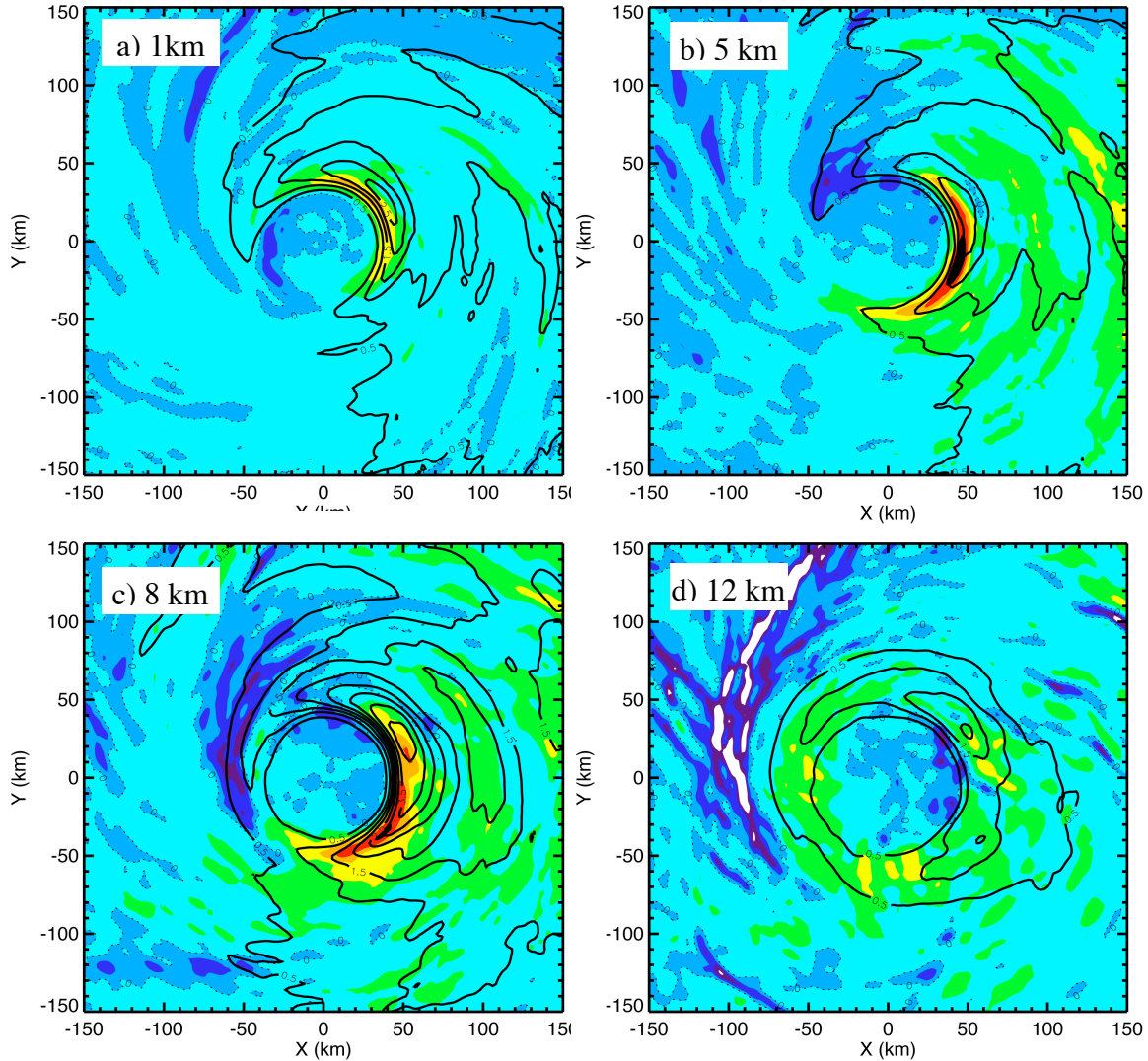
Figure 1. Time averaged fields of vertical motion (colors, intervals of 0.25 m s^{-1} for w<0, 0.5 m s^{-1} for w>0) and total precipitation mixing ratio (sum of rain, snow, and graupel, solid contours at intervals of 0.5 g kg^{-1}). Fields are 6-h averages using output every 3 min from hours 24-30 of the simulation.

asymmetry onto two types of vortex Rossby waves: sheared vortex Rossby waves, in which the radial shear of the swirling flow axisymmetrizes tilt asymmetries, and a quasi-mode, or discrete, vortex Rossby wave that causes precession of the upper part of a tilted vortex until it realigns with the lower part (thereafter undergoing repeated cycles of tilting and realignment).

To examine mechanism (1), the center position from the time-averaged fields was determined at each height and the results (not shown) indicate a south-eastward tilt of 6-8 km between heights of 1-12 km. Figure 1 therefore shows that the maximum upward motion at mid-to-upper levels occurs in the downtilt direction. Calculation of the center location at 8 km at every time for the 24-30 h period (not shown) further indicates precession of the upper vortex relative to the surface vortex, suggesting the presence of a quasi-mode vortex Rossby wave. The presence of sheared vortex Rossby

waves has not yet been investigated. These results suggest that the tilting of the vortex may play a role in the development of the asymmetry and further suggests that mechanism (2) does not. Mechanism (3) was examined by overlaying contours of horizontal divergence with contours of vorticity as well as wind vectors associated with the asymmetric wind (determined by subtracting out the azimuthally averaged tangential and radial winds). According to the vorticity balance argument, areas of negative (positive) vorticity advection should be associated with areas of convergence (divergence). The results (Fig. 2) indicate that regions with asymmetric inflow (outflow) in the eyewall are associated with convergence (divergence). The relative flow in the boundary layer (Fig. 2a) is from the northeast so that the maximum boundary layer convergence occurs on the northeastern side of the eyewall, thereby producing the upward motion maximum
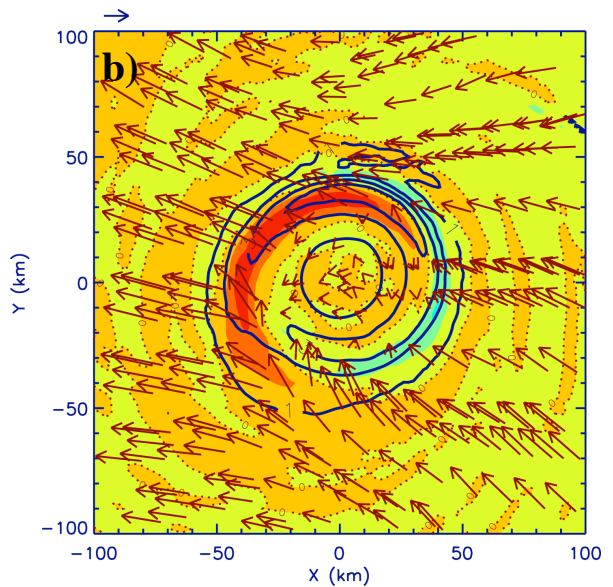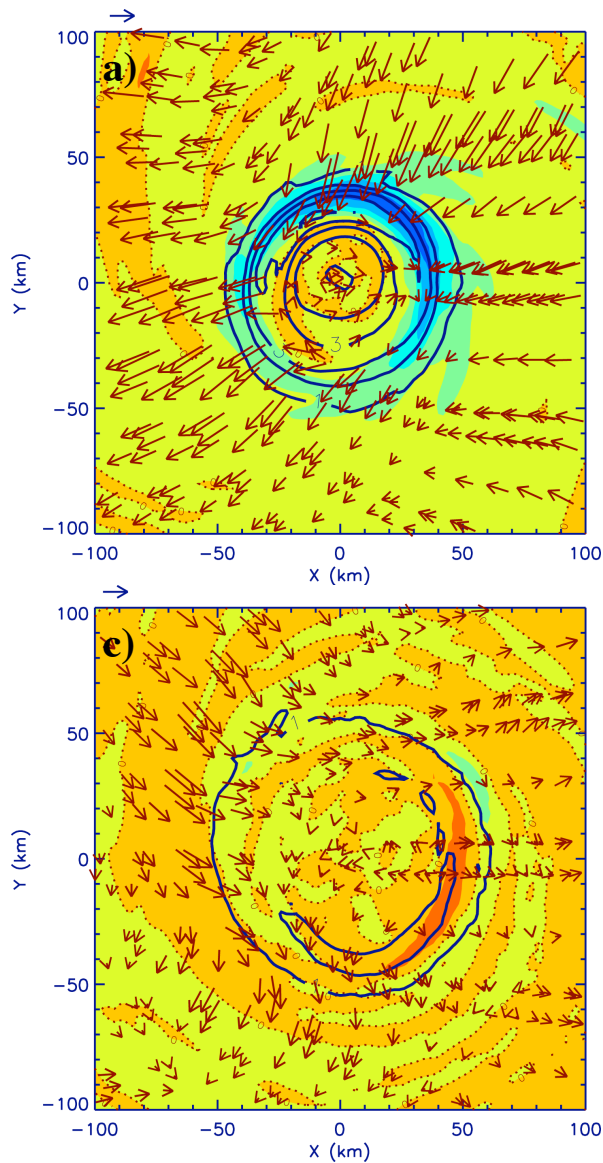
Figure 2. Horizontal cross sections of divergence (colors), vorticity (contours), and asymmetric winds at (a) 245 m, (b) 1.1 km, and (c) 8.2 km. The contour interval for divergence is 0.5×10^{-3} s^{-1}, with the zero contour highlighted by the dotted contours. For vorticity, the contour interval is 1×10^{-3} s^{-1} starting at 1×10^{-3} s^{-1}. The wind vector above the upper level corner corresponds to 5 m s^{-1}.

side and growing to maximum height on the northern side, but are instead seen to extend through the depth of the troposphere virtually from their inception. Also, the updrafts are seen to first develop at mid-upper levels (3-10 km) on the south-southwestern side of the storm and then to extend downward to near the top of the boundary layer on the southeastern side of the storm. This pattern of development can be seen in Fig. 1 by the shift in the location of upward motion between Fig. 1a and Figs. 1b and 1c.

To explain the mechanisms that control the timing and location of the updrafts, consider the distributions of radial velocity, vorticity, and upward motion at 1.1 km shown in Fig. 3. The relative flow at this level is from the southeast (Fig. 2b) such that the strongest inflow occurs on the southeastern side of the storm and outflow occurs on the northwestern side. In Fig. 3a, a ring of high vorticity is seen associated with the eyewall and within this ring are areas of highly concentrated vorticity, or mesovortices. Considering the mesovortex on the southeastern side, its circulation should produce relative outflow (inflow) on its trailing (leading) side, where the terms "trailing" and "leading" are defined in terms of the movement of the mesovortex cyclonically around the eyewall. The radial velocities show a region of weak outflow trailing the mesovortex and an area of inflow extending into the eye ahead of the mesovortex, consistent with this interpretation. Where the outflow meets with the general area of inflow, there is enhanced convergence and, in the area of vortex-induced inflow, there is reduced convergence. As a result, the enhanced convergence trailing the mesovortex leads to the formation of the updraft there (Fig. 3b).

there in Fig. 1a. Above the boundary layer, the relative flow produces low-level convergence (Fig. 2b) and upper-level divergence (Fig. 2c) on the southeastern side of the storm, thereby producing the maximum upward motion on that side of the eyewall at 5 and 8 km (Figs. 1b, 1c). Consequently, the pattern of upward motion at most levels can be explained by mechanism (3).

4. Updraft structure and eyewall mesovortices

Although the time-averaged vertical motion fields show a relatively smoothly varying asymmetric vertical motion pattern, the upward motion in the eyewall at any instant in time is typically comprised of one or more convective updrafts that occupy only a relatively small percentage of the eyewall area (as in Braun 2002). These updrafts are observed to form on the southern side of the eyewall and dissipate on the northern side, similar to the conceptual model of Heymsfield et al. (2001). However, in contrast to the conceptual model, the updrafts are not starting off shallow on the southern
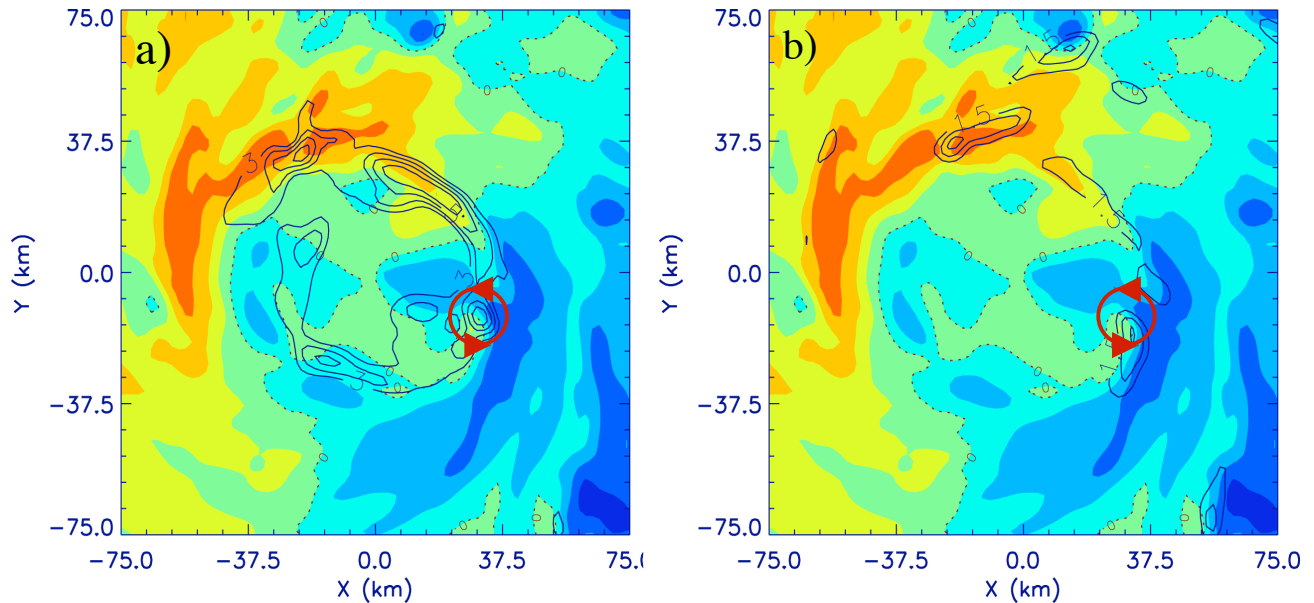
Figure 3. Horizontal cross sections of radial velocity at 1.1 km and (a) vorticity and (b) vertical motion. The implied circulation associated with the southeastern mesovortex is indicated. The contour interval for radial velocity is 5 m s^{-1}, with the zero contour highlighted by dotted contours. For vorticity, the contour interval is 1x10^{-3} s^{-1} starting at 3x10^{-3} s^{-1} while for vertical velocity the contour interval is 1 m s^{-1} starting at 1.5 m s^{-1}.

To show that this pattern exists at other times, Fig. 4 shows a Hovmoller diagram of the radially averaged absolute vertical vorticity and vertical velocity at 1.1 km. The vorticity field shows positive vorticity anomalies that rotate around the storm at least once and, in some cases, several times. When these positive vorticity anomalies move into the eastern half of the storm, updrafts form and slightly trail the vorticity anomalies in time in a given direction. Consider vorticity anomaly A in Fig. 4. It starts on the western side of the storm and initiates an updraft when it moves into the eastern side of the storm. It subsequently rotates around the storm, initiates a new burst of convection on the eastern side, and then rotates around again to eventually form a third round of convection. Vorticity anomaly B is associated with two episodes of convection before dissipating on the southwestern side of the storm. In some cases, such as vorticity anomaly C (formed by the merger of two vorticity anomalies), the vorticity appears to be generated by the convection and then subsequently moves around the storm to initiate a subsequent episode of convection. These results suggest a strong linkage between eyewall mesovortices and convective updrafts. Updrafts form when the mesovortices move into the region where the relative flow supports the upward component of the wavenumber 1 asymmetry in vertical motions.

Given this understanding that the updrafts form where the mesovortex interacts with the wavenumber 1 forcing of vertical motion, we are now in a position to explain why the updrafts form at mid-to-upper levels prior to forming near the top of the boundary layer. Within the boundary layer, the relative asymmetric flow produces maximum convergence on the northeastern side of the eyewall (Fig. 2a) so that the interaction of the mesovortex with this convergence pattern produces updrafts that form on the southeastern side of the storm and dissipate on the northwestern side. In contrast, above the boundary layer, the asymmetric flow produces low-level convergence (Fig. 2b) and upper-level divergence (Fig. 2c) on the southeastern side of the storm, allowing mesovortices to initiate updrafts on the south-southwestern side and later dissipate on the northeastern side of the storm.

The mesovortices form as a result of the breakdown of the ring of vorticity within the eyewall. As shown by Schubert et al. (1999) for the case with no vorticity forcing, a ring of vorticity is barotropically unstable so that small perturbations will grow rapidly allowing the axisymmetrization process to gradually change the ring of vorticity to a vortex monopole. In a storm with active convective forcing, the axisymmetrization process does not reach this final state of a vortex monopole because the convection maintains the ring of vorticity. Consequently, mesovortices are continually generated as the ring of vorticity breaks down as a result of barotropic instability but is maintained by convection. Montgomery et al. (2002) have shown that in the forced case, long-lived mesovortices can form and produce winds 50% greater than the parent vortex. In the simulation, peak winds at the top of the boundary layer are up to 40% larger than the azimuthally averaged values.

5. Summary

The numerical simulation of Bonnie suggests that updrafts in the eyewall are the result of the interplay between wavenumber 1 forcing of vertical motion and
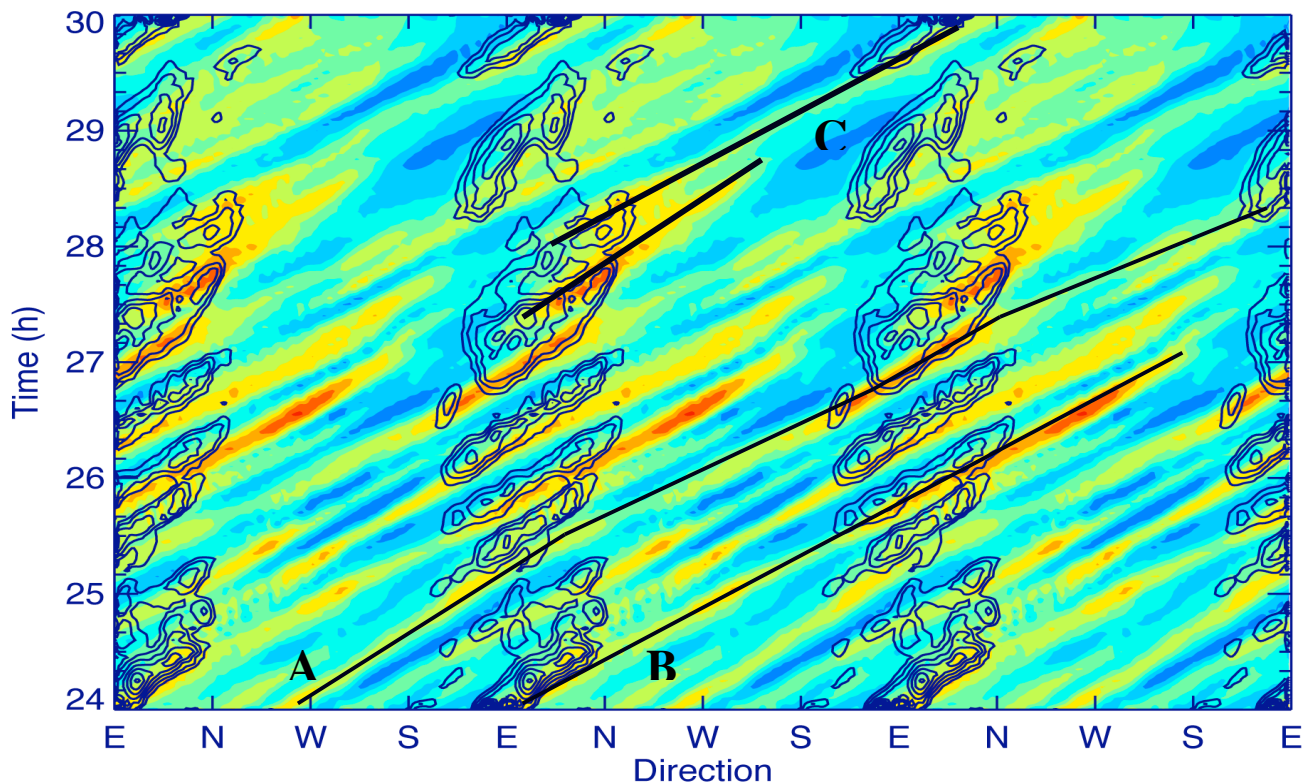
Figure 4. Hovmoller diagram of radially averaged (20-54 km) absolute vertical vorticity (colors, contour interval of 0.25×10^{-3} s^{-1} starting at 1.25) and vertical velocity (contour interval of 0.1 m s^{-1} starting at 0.6) at 1.1 km elevation. The plot has been extended to three revolutions around the center. Solid lines follow individual vorticity disturbances or mesovortices.

eyewall mesovortices. The wavenumber 1 forcing of vertical motion is consistent with the idea that horizontal vorticity advection is roughly balanced by the stretching or compression of vorticity such that convergence occurs in association with inflow into the eyewall and divergence occurs with outflow from the eyewall. The mesovortices, which rotate cyclonically around the eyewall, contribute to upward motions by producing enhanced (weakened) convergence on their trailing (leading) sides as they move into the favorable portion of the wavenumber 1 asymmetry.

References

Bender, M. A., 1997: The effect of relative flow on the asymmetric structure in the interior of hurricanes. *J. Atmos. Sci.*, **54**, 703-724.

Braun, S. A., 2002: A cloud-resolving simulation of Hurricane Bob (1991): Storm structure and eyewall buoyancy. *Mon. Wea. Rev.*, **130**, 1573-1592.

Frank, W. M., and E. A. Ritchie, 2001: Effects of vertical wind shear on the intensity and structure of numerically simulated hurricanes. *Mon. Wea. Rev.*, **129**, 2249-2269.

Garratt, J. R., 1992: *The Atmospheric Boundary Layer*, Cambridge University Press, 316 pp.

Heymsfield, G. M., J. Halverson, J. Simpson, L. Tian, and T. P. Bui, 2001: ER-2 Doppler radar (EDOP) investigations of the eyewall of Hurricane Bonnie during CAMEX-3. *J. Appl. Meteor.*, **40**, 1310-1330.

Jones, S. C., 1995: The evolution of vortices in vertical shear: Initially barotropic vortices. *Quart. J. Roy. Meteor. Soc.*, **121**, 821-851.

Montgomery, M. T., V. A. Vladimirov, and P. V. Denissenko, 2002: An experimental study on hurricane mesovortices. *J. Fluid Mech.*, **471**, 1-32.

Pagowski, M., and G. W. K. Moore, 2001: A numerical study of an extreme cold-air outbreak over the Labrador Sea: Sea Ice, air-sea interaction, and development of polar lows. *Mon. Wea. Rev.*, **129**, 47-72.

Pu, Z., and S. Braun, 2001: Evaluation of bogus vortex techniques with four-dimensional variational data assimilation. *Mon. Wea. Rev.*, **129**, 2023-2039.

Reasor, P. D., M. T. Montgomery, and L. D. Grasso, 2003: A new look at the problem of tropical cyclones in vertical shear flow: Vortex resiliency. *J. Atmos. Sci.*, (submitted).

Schubert, W. H., M. T. Montgomery, R. K. Taft, T. A. Guinn, S. R. Fulton, J. P. Kossin, and J. P. Edwards, 1999: Polygonal eyewalls, asymmetric eye contraction, and potential vorticity mixing in hurricanes. *J. Atmos. Sci.*, **56**, 1197-1223.

Wang, Y., and G. J. Holland, 1996: Tropical cyclone motion and evolution in vertical shear. *J. Atmos. Sci.*, **53**, 3313-3332.